Adsorption of 4-Picoline and Piperidine to the Hydrated SiO$_2$ Surface: Probing the Surface Acidity with Vibrational Sum Frequency Generation Spectroscopy

DINGFANG LIU, GANG MA, AND
HEATHER C. ALLEN*

*Department of Chemistry, The Ohio State University,
100 West 18th Avenue, Columbus, Ohio 43210*

Vapor adsorption is an important process influencing the migration and the fate of many organic pollutants in the environment. In this study, vibrational sum frequency generation (SFG) spectroscopy was used to study the adsorption of two surface acidity probe molecules, 4-picoline (pK_a = 5.94) and piperidine (pK_a = 11.24), onto the amorphous SiO$_2$ surface. The adsorption of 4-picoline onto the silica surface occurs by forming weak hydrogen bonds between the nitrogen atoms of 4-picoline molecules and the hydrogen atoms of surface silanol OH groups. Piperidine molecules are strongly chemisorbed onto the SiO$_2$ surface through the protonation of piperidine molecules by surface silanol OH groups. The SFG results indicate that the surface acidity constant of silanol OH groups (pK_a-(HOSi≡)) is in the range of 5.94–11.24 at the air/solid interface. Although this range of surface acidity constants is quite wide, it is possible to narrow it by choosing probe molecules with a smaller pK_a range. Together with theoretical prediction methods, adsorption studies using vibrational SFG spectroscopy are capable of quantifying the surface acidity of mineral oxides by carefully choosing the acidity probe molecules.

Introduction

Most geochemical and environmental reactions under ambient temperature occur at solid/water and solid/gas interfaces (*1*). The adsorption of organic vapor onto mineral oxide surfaces is one of the most important factors governing the mobility and distribution of volatile organic compounds (VOCs) in the unsaturated soil zone. In the troposphere, the heterogeneous reactions between mineral aerosol and organic gases are critical for governing the trace atmospheric gas budget (such as O$_3$) (*2*, *3*). However, it is complicated to study the interaction between the organic molecules and soil surfaces in the natural environment because there are many interrelated factors that play important roles in the behavior of both sorbents and sorbates(*4*). Therefore, it is necessary to study the interaction between sorbate molecules and soil mineral particles by using model systems.

It is well-known that the silica surface is fully hydroxylated in the soil environment with a point zero charge (PZC) range of 2–4 (*5*, *6*). Numerous spectral and chemical data have unambiguously confirmed the presence of OH groups on the silica surface from different sources (*7*, *8*). Surface silanol groups play a key role in sorption processes that involve physical and/or chemical bonding forces, that is, physisorption and chemisorption, respectively. Sorbate molecules bound through chemisorption (e.g. inner sphere complexes at the liquid/solid interface) are different chemical entities than if bound through physisorption (e.g. outer sphere complexes or presence in the diffuse part of the double layer at the liquid/solid interface). Therefore, it is important to distinguish between physisorption and chemisorption. Direct evidence for chemisorption comes from spectroscopic methods, such as vibrational (*9*, *10*) or synchrotron-based in-situ X-ray absorption (*11*) spectroscopic techniques. In this study, vibrational sum frequency generation (SFG) spectroscopy was used to investigate the adsorption properties and the surface acidity of the amorphous silica surface.

Surface complexation theory incorporates the chemical and physical structure of the electrical double layer into a theoretical model that assumes that surface reactions mimic aqueous complexation (*6*, *12*). Intrinsic surface acidity constant (pK_a^{int}) values, electrostatic parameters, and even site densities are fit from potentiometric titration data. This abundance of fitted parameters can cause the unfortunate consequence that any number of models can be made to predict titration data accurately (*13*, *14*). Recent approaches have been made to reduce the number of fitted parameters in surface complexation models by the theoretical estimation of the distribution of sites and surface pK_a^{int} values for different types of functional groups. As one of the most successful and popular methods, the bond-valence method correlates the surface acidity of mineral oxides with their metal cation hydrolysis constants in aqueous solution (*13*, *15*). Since the correlation involves the bond length of surface functional groups, Bickmore et al. obtained the bond length information from a more realistic relaxed surface structure determined by using ab initio surface structure optimizations (*13*) instead of using bond lengths from the rigid crystalline structure. Their predictions of pK_a^{int} values were 11.6 for the gibbsite (100) surface, 11.5 for the gibbsite (010) surface, and 5.5–8.4 for the cristobalite (100) surface. The rationale of these predicted values are generally tested indirectly by comparing with measured pH$_{pzc}$ values (pH$_{pzc}$ = $^1/_2$(pK_{a1}^{int} + pK_{a2}^{int})). However, it is possible to directly test the rationale of predicted surface acidity constants by using spectroscopy methods with carefully chosen probe molecules.

To understand the chemical processes (e.g. adsorption, desorption, and heterogeneous catalysis of controlled or natural environments) on mineral oxide surfaces, it is very important to obtain quantitative information of their surface acidities (*16*). Surface acidity properties of hydroxyl groups on metal oxide surfaces are generally characterized by using vibrational spectroscopic methods to study the interaction with basic molecules, such as piperidine, pyridine, ammonia, and picoline. The adsorption of pyridine as a tool to test the acidity of oxide surfaces has been proposed long ago (*17*), and this molecule has the demonstrated capability to distinguish between Lewis and Brønsted acidity, giving rise to specific infrared (IR) absorption bands (*18*, *19*). For silica surfaces, many studies indicated that there is only hydrogen-bond formation between surface silanol OH groups and weakly basic probe molecules such as pyridine (*20*, *21*). These studies suggest there are no Brønsted or Lewis acidity sites on the SiO$_2$ surface. Molecular dynamic simulation (gas-phase approach) on proton binding to the silica surface predicts a surface pK_a of 8.5 for the reaction ≡SiOH → ≡SiO$^-$

* Corresponding author phone: 614-292-4707; fax: 614-292-1685; e-mail: allen@chemistry.ohio-state.edu.

+ H^{+} (22). However, an IR spectroscopic study found that surface silanol groups are shown to deprotonate due to the adsorption of basic molecules, such as ammonia, pyridine, or 2,6-dimethylpyridine after addition of gases such as SO_2 or NO_2 (23). In this study, two basic molecules, 4-picoline ($pK_a = 5.94$, relatively weak base) and piperidine ($pK_a = 11.24$, relatively strong base), were used as surface acidity probe molecules, and their adsorption properties were investigated by a surface specific vibrational spectroscopic technique, surface vibrational SFG spectroscopy.

Sum frequency generation is a second-order nonlinear process that utilizes a high-intensity electric field from a laser source. Lack of inversion symmetry at air/liquid, air/solid, and liquid/solid interfaces makes SFG inherently surface sensitive. The SFG spectrum can provide useful molecular level information about molecular orientation, conformation at the surface, and surface structure (24, 25). SFG spectroscopy shows great promise in studying environmental interfaces with application in the environmental geochemistry area (2, 3, 26). The theory of SFG can be found in other publications (25, 27−29). Here, a brief introduction of sum frequency generation spectroscopy is provided in the Supporting Information.

Experimental Section

Sum Frequency Generation. This study employed two types of SFG systems, a state-of-the-art broad bandwidth SFG (BBSFG) system and a scanning SFG system. Since the BBSFG system typically provides better spectral signal-to-noise ratios than the scanning system, it was used to investigate the C−H stretching region of adsorbed piperidine. The detailed description of the SFG systems can be found in previously published research papers (30−35) and is also included in the Supporting Information. The spectra presented here are the average of at least two replicate spectra. The spectra were acquired at the ambient condition of 23 ± 1 °C and a relative humidity (RH) of 54 ± 2% with a 5-min CCD acquisition time (BBSFG) and a 20−50 min acquisition time (scanning SFG: 10−30 s exposure time for each data point).

SFG spectra interpretation must be conducted after deconvolution into the component peaks since direct comparison of SFG spectra to Raman and IR spectra may be misleading. The details of the curve-fitting method were reported previously (36).

Raman. The Raman experimental setup consists of a 532-nm CW laser (Spectra-Physics, Millennia II), a 5-mm focusing Raman probe (InPhotonics, RP 532-05-15-FC), a 500-mm monochromator (Acton Research, SpectraPro SP-500) using a 600 g/mm grating, and a back-illuminated CCD (Roper Scientific, LN400EB, 1340 × 400 pixel array and deep depletion). Raman spectra were collected using a fiber optic, which was coupled to the entrance slit of the monochromator through a fiber optic imaging coupler (Acton Research, FC-446-030). SpectraSense software (Acton Research version 4.1.9) was used for data collection and display. The power of the 532-nm beam for sample illumination was 90 mW. Before data collection, the Raman system was calibrated by using the 435.83 nm line of a fluorescence lamp and was verified by comparison to the Raman spectrum of naphthalene. The Raman spectral resolution and acquisition temperature were 0.8 cm^{−1} and ~23 °C. The sample was placed in a glass vial. The sample glass vial was placed in a home-built sample holder, which holds the sample vial and the Raman probe. The alignment of the Raman probe in the sample holder can affect the detected Raman intensity to some extent. The intensity variation can be normalized by taking a Raman spectrum of a reference sample (i.e. neat piperidine in this study) when comparison of the Raman intensity between different samples is necessary.

FTIR. A Thermo Nicolet FT-IR spectrometer (Avatar 370, Thermo Electron Corp.) was employed in the FTIR spectroscopy experiments. The spectrometer is equipped with DTGS KBr detector and purged with hydrocarbon-, H_2O-, and CO_2-free air. Spectra were collected with a spectral resolution of 4 cm^{−1} and 128 scans at a temperature of ~24 °C. A demountable IR cell equipped with a pair of CaF_2 windows was utilized. The second-derivative method is used to obtain the positions of the overlapped peaks in the FTIR spectrum as a resolution enhancement technique.

Materials and Chemicals. The infrared-grade fused silica plates were purchased from Quartz Plus Inc. According to the manufacturer data, the surface quality is 60−40, flatness ~ 5 waves, parallelism < 15 min, surface roughness = 1.5−3 nm, and bulk hydroxyl content ≤ 8 ppm. Before the SFG experiments, silica plates were annealed in a muffle oven (Fisher Scientific, Isotemp muffle furnace) at 900 °C for more than 12 h in order to remove possible organic contamination. After the silica plates were cooled to room temperature, they were kept under ambient conditions for more than 30 min to allow equilibrium with the water vapor in the air. Then, SFG experiments were performed on the silica surface before and after the vapor adsorption. The adsorption experiments were completed by placing the oxide into a sealed bottle with saturated organic vapor for 10 min and then purged with organic free air to the silica surface for 2 h. The silica plates were then placed back onto the sample stage to investigate the air−solid interface by SFG spectroscopy.

Piperidine and 4-picoline were purchased from Aldrich Chemicals and used as received. Deionized water was obtained from a Millipore Nanopure system (18.3 MΩ·cm).

Results and Discussion

4-Picoline at the Air/Liquid Interface. The SSP-polarized SFG spectra of 4-picoline ($C_5H_4NCH_3$) at the air/liquid and air/solid interfaces are shown in Figure 1. 4-Picoline is a surface-active compound with a hydrophilic pyridine end and a hydrophobic alkyl end. These moieties are well-represented in the SFG spectra of 0.01 mole fraction (mf) 4-picoline aqueous solution (Figure 1a). The spectrum reveals a strong SFG response from the methyl group and a minimal SFG response from the free OH stretch of water molecules (3700 cm^{−1}), which is suppressed by forming hydrogen bonds with the hydrophilic nitrogen of 4-picoline molecules. The broad bands in the 3000−3600-cm[−1] region contain the hydrogen-bonded OH stretching peaks. Two prominent peaks are observed in the CH stretching region. On the basis of previous infrared and Raman peak assignments (37−39), the peak around 2875 cm^{−1} is attributed to CH_3 symmetric stretch (CH_3-SS) modes, and the peak around 2930 cm^{−1} is due to CH_3 antisymmetric stretch (CH_3-AS) modes. Since 4-picoline has one methyl group at the γ-position of the pyridine ring, the molecular orientation information of 4-picoline at the air/liquid interface can be obtained by comparing CH_3 stretches in SFG spectra acquired with different polarization combinations. The SFG spectra of 0.01 mf 4-picoline at the air/liquid interface were acquired with SSP and SPS polarization configurations. The SFG intensity of the CH_3-SS peak around 2875 cm^{−1} is minimal for the SPS polarization combination compared to that of the SSP polarization combination. The molecular orientation information at the air−liquid interface was obtained by analyzing the SFG response ratio (40, 41) of the CH_3-SS at different polarization configurations (SSP vs SPS) and then confirmed by comparing the SFG response ratio between the CH_3-SS and the CH_3-AS in the SSP polarization configuration. The orientation-angle calculation for the CH_3 vibrational modes (details in the Supporting Information) suggests that the orientation distribution of the methyl group is tilted from
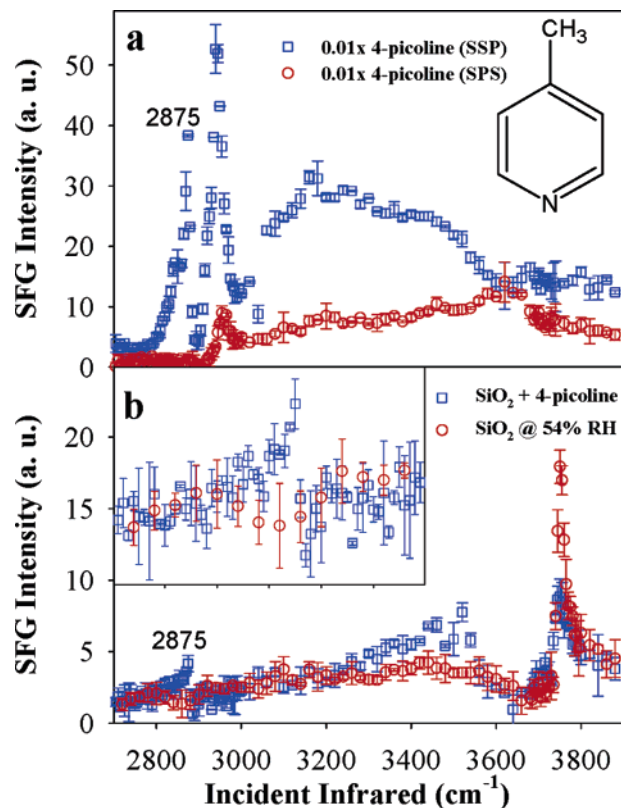
FIGURE 1. (a) The SFG spectra of 0.01 mf 4-picoline at the air/liquid interface and (b) SiO₂ at the air/solid interface before and after exposure to 4-picoline vapor at 54% relative humidity. The inset in part b is the enlarged spectrum in the CH stretching region (2700–3000 cm⁻¹).

the sample surface. Moreover, at the air/liquid interface, the hydrophilic end of 4-picoline molecules likely interacts with the water molecules by forming hydrogen bonds between nitrogen atoms of 4-picoline molecules and hydrogen atoms of water molecules, while the hydrophobic methyl end points away from the liquid surface.

4-Picoline Adsorption on the Amorphous Silica Surface. As discussed in our previous work (*36*), at 54% RH, the SFG spectrum (Figure 1b) of the air/silica interface reveals weak hydrogen-bonded OH stretching bands, and a strong isolated silanol OH stretching peak around 3750 cm⁻¹. This indicates that water molecules only cover a limited portion of the hydrated silica surface, and the isolated silanol OH group is the major surface species. As shown in Figure 1b, the CH_3 stretching peaks suggest that adsorption of 4-picoline occurred on the silica surface. This adsorption of 4-picoline causes a significant suppression (half of the intensity) of the silanol OH stretching peak. However, there is no CH_3 stretching SFG signal detected after purging the 4-picoline adsorbed silica plate for 24 h with organic-free nitrogen gas. In addition, the isolated silanol OH peak intensity recovered to approximately the same intensity as that of the silica surface without 4-picoline vapor exposure. This further demonstrates that the 4-picoline on the silica surface is physisorbed. Physisorption is weak and reversible adsorption, whereas chemisorption is often strong and chemically bound. In summary, the adsorption of 4-picoline onto the silica surface occurs by forming weak hydrogen bonds between nitrogen atoms of 4-picoline molecules and hydrogen atoms of isolated silanol OH groups. These results are in agreement with FT-IR studies, which concluded that the hydrogen-bond formation between adsorbate molecules and hydrogen atoms of surface silanol groups plays a major role in the adsorption of organic molecules from the vapor state (*7, 42*).
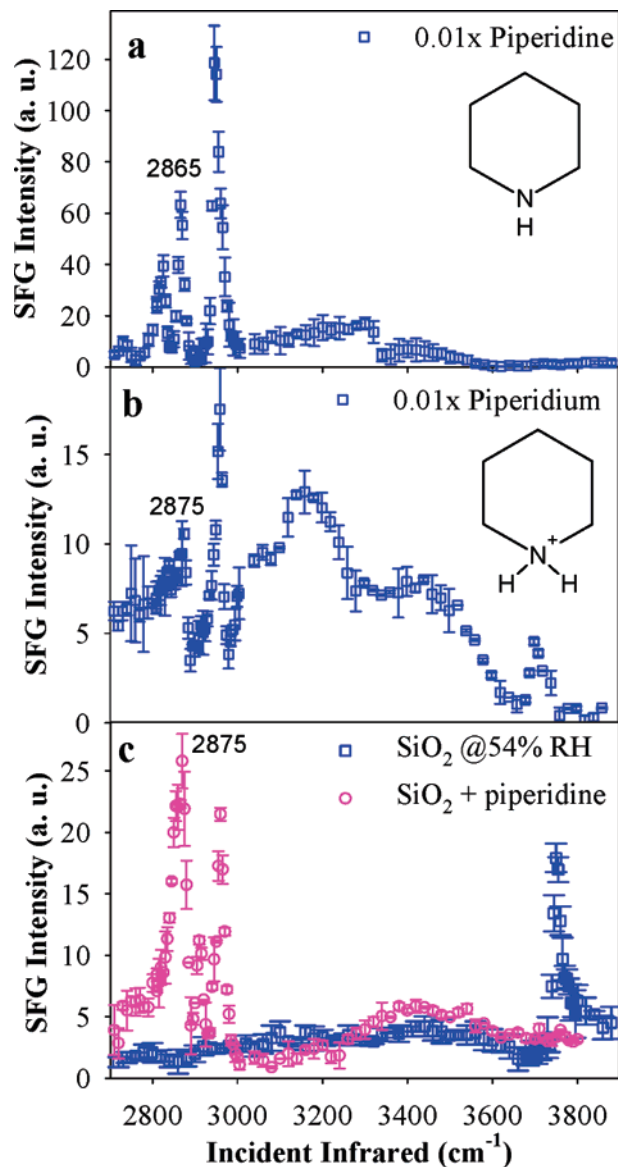

FIGURE 2. (a) The SFG spectra of 0.01 mf piperidine at the air/liquid interface, (b) 0.01 mf piperidium at the air/liquid interface, and (c) SiO₂ at the air/solid interface before and after exposure to piperidine vapor at 54% relative humidity.

Piperidine and its Protonation Product at the Air/Liquid Interface. The SFG spectra of 0.01 mf piperidine ($C_5H_{10}NH$) and piperidium chloride (protonated piperidine cation with a chloride anion, $C_5H_{10}NH_2Cl$) are shown in Figure 2a,b. Similar to 4-picoline, piperidine is also a surface-active compound. The SFG spectrum of 0.01 mf piperidine aqueous solution (Figure 2a) shows a strong CH_2 stretching response, while the free OH stretch of water molecules (3700 cm⁻¹) completely disappears. This suggests that piperidine is hydrogen-bonded with water at the amine end, leaving the hydrophobic alkyl end extruding toward the air phase. As shown in Figure 2, the broad peaks in the 3000–3600-cm⁻¹ region include both the hydrogen-bonded OH stretching peaks and the NH stretching peaks. Since these peaks are broad and overlap with each other, it is difficult to extract useful information from this region. However, the spectrum clearly shows that the protonation changes the NH stretching peak position from ∼3300 cm⁻¹ (Figure 2a) for piperidine to ∼3150 cm⁻¹ (Figure 2b) for piperidium.

Protonation reduces the surface activity of piperidium, as shown in Figure 2b. The SFG signal intensity of the CH_2
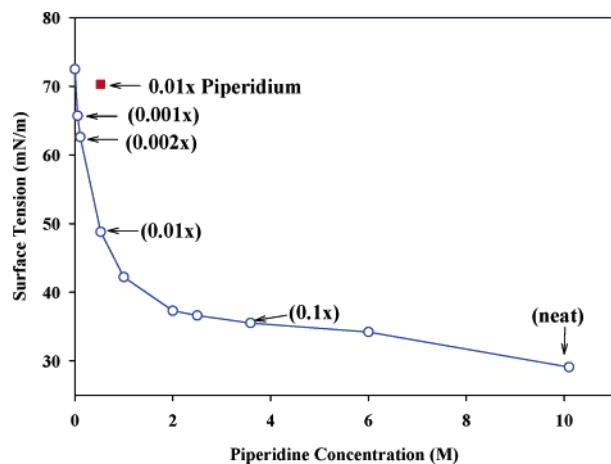
FIGURE 3. The surface tension of piperidine aqueous solutions (open circles), and the surface tension of 0.01 mf piperidium (solid square).

stretch peaks for 0.01 mf piperidium aqueous solution decreases to approximately one-eighth of the SFG intensity for 0.01 mf piperidine. One should be careful to make conclusions by comparing only the SFG intensities in the CH stretch region, since SFG intensity is proportional to the number density of the molecules as well as the molecular orientation at the interface. However, the small free OH stretching peak shown in Figure 2b indicates that a portion of the surface water molecules are not bonded with piperidium molecules. This somewhat justifies the comparison of the surface coverage for 0.01 mf piperidine and piperidium aqueous solutions. The SFG spectrum of 0.01 mf piperidine (Figure 2a) suggests full surface coverage of piperidine molecules, which occupy all the free OH of water by forming hydrogen bonds. In addition, suppression of the hydrogen-bonded region of surface water is observed for the SFG spectrum of piperidine aqueous solution. Therefore, by comparing the SFG results in both CH and OH stretching regions, protonation of piperidine causes a decrease in its number density at the air/liquid interface. The surface tension measurements (Figure 3) further confirm this result by revealing a larger decrease of surface tension for piperidine aqueous solution relative to that of piperidium. The surface tension decreases substantially at low concentrations of piperidine. Whereas, surface tension of 0.01 mf piperidium (protonated piperidine) (red solid square) decreases only slightly to 70.3 mN/m compared to the significant decrease for the 0.01 mf piperidine aqueous solution (48.8 mN/m). The relatively small decrease in surface tension for piperidium may be due to solvation enhancement after protonation.

Piperidine Adsorption on the Amorphous Silica Surface. The strong SFG response from the CH_2 stretching modes as shown in Figure 2c indicates the adsorption of piperidine molecules on the SiO_2 surface. The silanol OH stretch peak at 3750 cm^{-1} is completely suppressed by the adsorption of piperidine molecules. This reveals that the adsorption of piperidine onto the SiO_2 surface occurs through the interaction between silanol OH groups and piperidine molecules. There are three possible scenarios that can cause the complete disappearance of the isolated silanol OH stretch peak as shown schematically in Figure 4. In the first scenario, piperidine molecules form a liquidlike layer on the SiO_2 surface, and the liquidlike layer completely covers the spectral information buried underneath. If this was true, the SFG spectrum of piperidine adsorbed on the SiO_2 surface should be similar to that of neat piperidine at the air/liquid interface. In the second scenario, piperidine molecules (proton acceptors) form hydrogen bonds with isolated silanol OH groups and occupy all the OH sites. In the third scenario,

piperidine molecules are protonated by surface silanol OH groups and form ≡Si−O−piperidium complexes through ionic bonds. This scenario is highly probable because piperidine is a relatively strong base with a pK_a value of 11.24 for its conjugated acid, and the reported pK_a (7) values for surface silanol OH groups are generally less than 9.0.

Similar to our previous study of piperidine adsorption to the hydrated α-Al_2O_3 (0001) surface (43), a piperidine vibrational mode (CH_2 symmetric stretch at ~2860 cm^{-1}) is used here as a spectroscopic probe to elucidate the true adsorption mechanism. Possible adsorption scenarios are shown in Figure 4. (N−H stretch vibrations are not used since these peaks overlap with O−H stretching peaks. In addition, the N−H of piperidine also takes part in hydrogen bonding which broadens the peaks.) Recall that the vibrational frequency provides information on the strength of the chemical bond, which is influenced by the chemical environment. If we can identify the frequency shifts of piperidine C−H stretching vibrations upon piperidine forming hydrogen bonds or upon protonation, it is possible to distinguish among the liquid-like piperidine, the hydrogen-bonded piperidine, and the protonated piperidine adsorption scenarios.

Seven peaks were used to fit both IR and Raman spectra as shown in Figure 5, and the peak positions obtained by the second-derivative technique (IR spectrum) are listed in Table 1. The spectral assignments for neat piperidine peaks are based on previous studies (44−47). Our previous Raman and SFG spectroscopy study (43) found that the protonation of piperidine molecules causes blue-shifting of a CH_2 symmetric stretch peak at 2854 cm^{-1}. Therefore, this same peak can be used as a probe peak for the protonation of piperidine molecules.

A BBSFG spectroscopy system was used in this study to take advantage of its higher spectral signal to noise ratios in the C−H stretch region. Figure 6 shows the BBSFG spectra of the air/liquid interface of neat piperidine, 0.01 mf piperidine and piperidium aqueous solution, and the air/solid interface of piperidine adsorbed on the SiO_2 surface. BBSFG spectra were fitted with Lorentzian profiles, and component peak positions are listed in Table 1. The CH_2 symmetric stretch reference peak blue-shifts from 2857 cm^{-1} for neat piperidine to 2862 cm^{-1} for 0.01 mf piperidine aqueous solution [partially protonated (<10% by calculation) in the aqueous environment] and ultimately blue-shifts to 2874 cm^{-1} for fully protonated piperidine aqueous solution (0.01 mf piperidium). For the BBSFG spectrum of piperidine adsorbed on the SiO_2 surface, the peak position of the protonation probe peak is ~2874 cm^{-1}, which is approximately the same as that of 0.01 mf piperidium (protonated piperidine) aqueous solution. This strongly suggests that the piperidine molecules adsorbed on the SiO_2 surface are protonated. In addition, we have exposed the piperidine adsorbed silica plate with HCl vapor to further protonate piperidine molecules adsorbed on the SiO_2 surface (if there are any piperidine molecules that are not protonated by silanol OH sites). The BBSFG spectra did not change before and after HCl exposure. This further confirms that the piperidine molecules adsorbed on the SiO_2 surface are protonated by the surface silanol OH sites.

To ensure that the significant SFG response shown in Figure 6d is from the monolayer of the protonated piperidine−silanol complex, a series of BBSFG spectra was acquired. These spectra were obtained after purging the piperidine-adsorbed SiO_2 plate with organic-free nitrogen gas for 0 h (Figure 7a), 0.25 h (Figure 7b), 2.5 h (Figure 7c), and 24 h (Figure 7d), respectively. The 0 h spectrum was obtained with the SiO_2 plate in an airtight sample cell filled with piperidine vapor. All the nitrogen-purged spectra were acquired in a sample cell filled with nitrogen gas. The probe peak position of the 0 h spectrum is the same as that of the
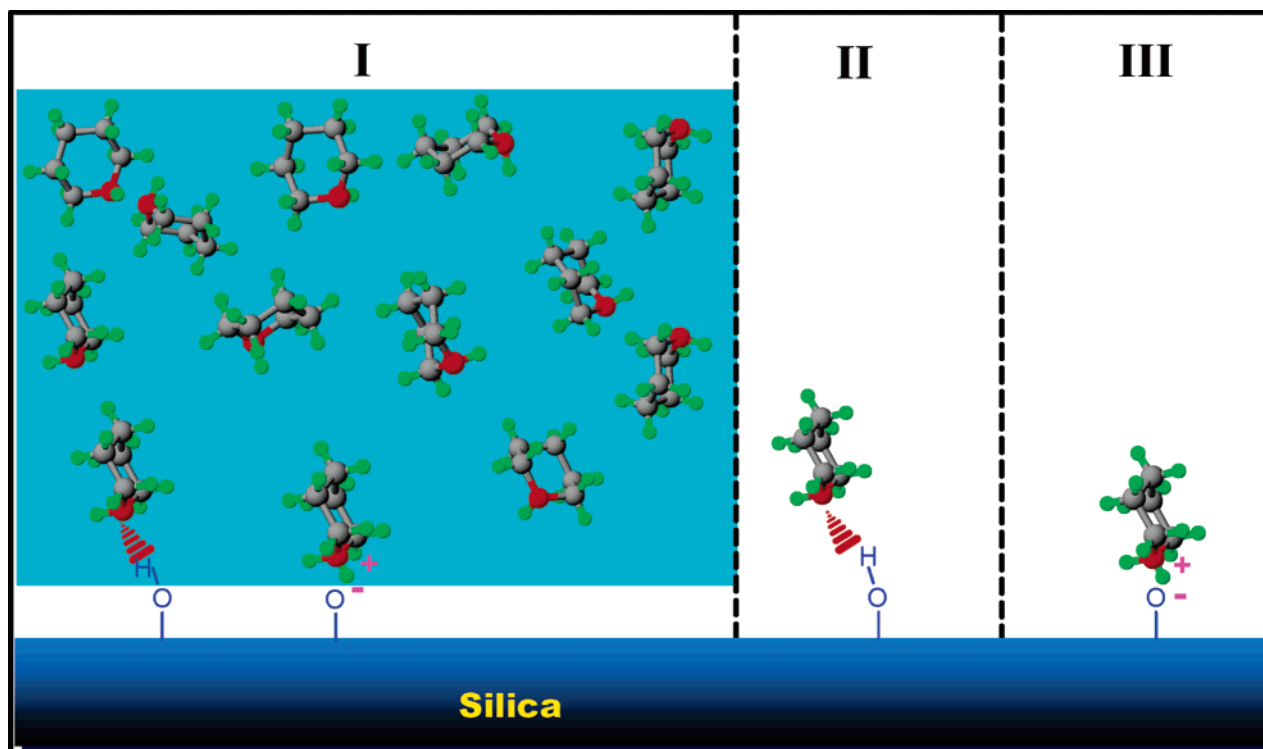
FIGURE 4. Schematic representation of piperidine adsorption scenarios. In the diagram, green spheres are hydrogen atoms, gray spheres are carbon atoms, and red spheres are nitrogen atoms. Scenario I, piperdine adsorbs to the silica surface by forming liquidlike layers; scenario II, hydrogen bond forms between piperidine and the surface OH group; scenario III, piperidine is protonated by the surface OH group.
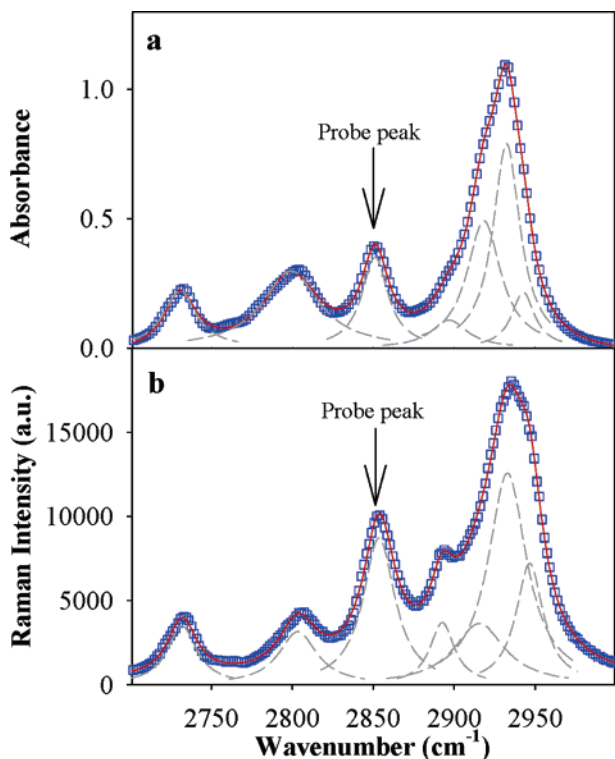

FIGURE 5. (a) FTIR and (b) Raman spectra of neat piperidine; blue squares, experimental; short dashed lines, Lorentzian component peaks; red solid line, overall fit.

neat piperidine SFG spectrum at the air/liquid interface. This suggests that a liquidlike layer of piperidine forms on the SiO_2 surface under the piperidine vapor environment. After purging with organic-free nitrogen gas, the probe peak position is gradually blue-shifted until after purging for 24

h. No significant change was found for longer purging times (36 and 48 h). The spectrum obtained after 24 h purging (Figure 7d) is similar to spectrum of silica after exposure to piperidine vapor for 10 min and then purging for 2 h (Figure 6d). This suggests that the piperidine molecules adsorbed on the SiO_2 surface are strongly bonded. In addition, the significant SFG response is due to the piperidine−silanol complex as opposed to the interaction of piperidine with piperidine or piperidine with H_2O.

Surface Acidity of the Amorphous Silica Surface. We observe an acid/base reaction chemisorption mechanism for the adsorption of piperidine on the silica surface. This is not observed for the adsorption of 4-picoline on the silica surface. Thus, the surface acidity strength of the silanol OH functional groups is between that of the conjugated acids of 4-picoline and piperidine according to acid/base (Brønsted) reaction theory. The measure of the strength of an acid relative to H_2O (the universal solvent) as a proton donor is given by the acid equilibrium constant (K_a, $-\log K_a = pK_a$) for the proton-transfer reaction (*5*, *6*). 4-Picoline is a weak base with pK_a of 5.94 for its conjugated acid (protonated 4-picoline), and piperidine is a relatively strong base with pK_a of 11.24 for its conjugated acid (piperidium or protonated piperidine). Therefore, the pK_a value of the surface silanol OH fuctional groups is between 5.94 and 11.24. In this study, we have used two organic probe molecules to investigate the surface acidity of the fused silica probed by using SFG spectroscopy, a surface-selective technique. Thus, using SFG, it is possible to determine the surface acidity experimentally for a flat, well-defined mineral surface with a relatively small surface area.

Previously, infrared absorption spectroscopy has been used as the major surface acidity probe technique (*48*); however, IR is typically used on particulate samples of which surfaces are not well defined in mineralogy terms. Surface acidity probe molecules that have been studied for quantifying the surface acidity of silanol OH groups by using infrared

TABLE 1. Spectra Fitting Results and Assignments

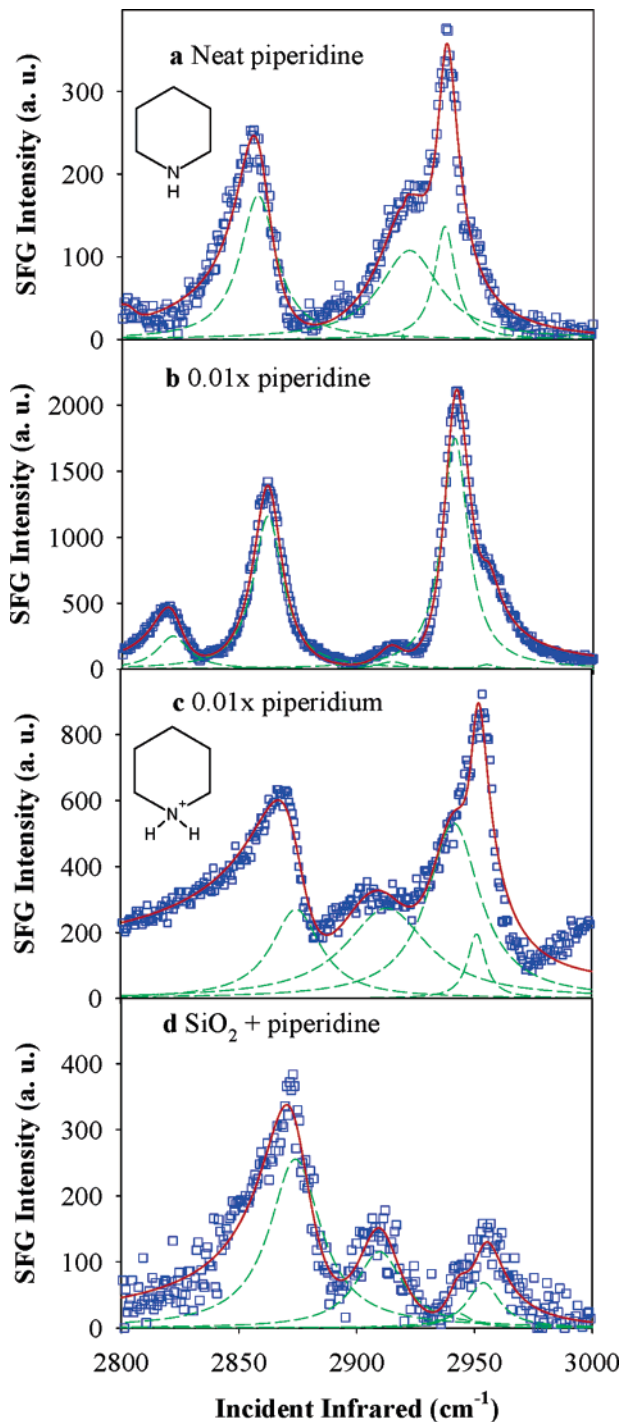|		CH₂-SS (cm⁻¹)			CH₂-AS (cm⁻¹)			
FTIR	neat piperidine	2730	2799	2851	2897	2918	2932	2943
Raman	neat piperidine	2732	2803	2854	2893	2916	2933	2947
BBSFG	neat piperidine		2803	2857		2919	2922	2937
BBSFG	0.01 mf piperidine		2821	2862		2914	2941	2954
BBSFG	0.01 mf piperidium			2874		2912	2941	2951
BBSFG	SiO₂-piperidine			2874		2909	2942	2953

FIGURE 6. BBSFG spectra of (a) neat piperidine, (b) 0.01 mf piperidine aqueous solution, (c) 0.01 mf piperidium aqueous solution, and (d) piperidine adsorbed on the SiO₂ surface. The solid red lines are overall fits, and the dashed green lines are component peaks.
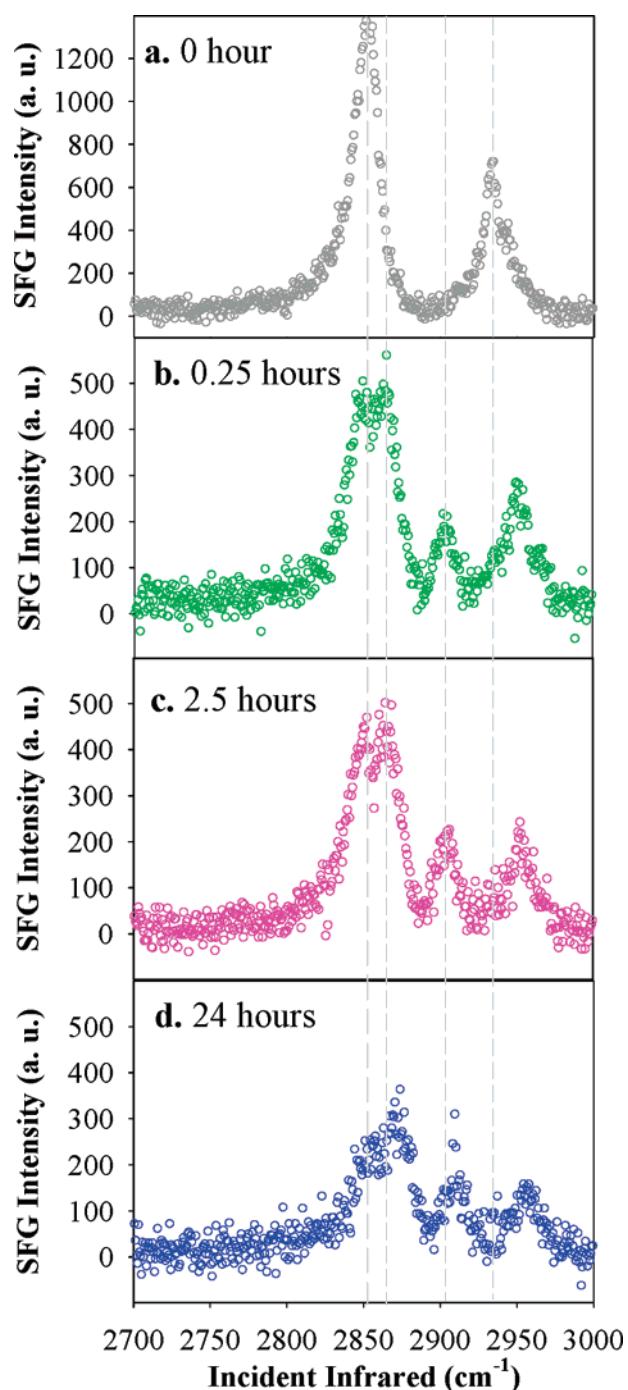

FIGURE 7. BBSFG spectra of piperidine on the SiO₂ surface. These are (a) the spectrum acquired under a piperidine vapor environment and spectra acquired under a nitrogen atmosphere and the sample purged with nitrogen gas for (b) 0.25 h, (c) 2.5 h, and (d) 24 h.

absorption spectroscopy include 2,6-dimethylpyridine (pK_a = 6.67) (19), 4-vinylpyridine (pK_a = 5.39) (48), pyridine (pK_a = 5.32) (20, 49), 2-vinylpyridine (pK_a = 4.95) (48), quinoline (pK_a = 4.90) (50), 2-chloropyridine (pK_a = 0.70) (51), diazines (pyrazine (pK_{a1} = 0.65), pyrimidine (pK_{a1} = 1.24), pyridazine

($pK_{a1} = 2.24$)) (52), and N-methylpyrrole ($pK_a = -2.90$) (53). Although the SiO_2 materials used in these IR studies have different forms, surface areas, sources, and pretreatment methods, conclusions from these studies are consistent with each other. That is, no Brønsted or Lewis acidity was observed for the silanol OH groups on the silica surface, and adsorption occurs by hydrogen-bond formation between probe basic molecules and surface silanol OH groups. However, none of these studies has used a basic probe molecule with a pK_a value higher than 7. As another alternative method, solid-state NMR technique (^{15}N cross-polarization magic angle spinning (CPMAS)) has been used with pyridine-^{15}N as the probe molecule (49). An adsorption study of mesoporous silica suggests that an acid site with a pK_a value of 2.8 is needed to form a quasisymmetric complex in the solid state with approximately equal bond lengths of OH (silanol OH) and NH (protonated pyridine-^{15}N) (49).

The results presented here are consistent with the pK_a values of the silica surface predicted by the bond valence method and values from Hiemstra et al. (7.9) (15) and from Bickmore et al. (8.5) (13). Both calculated pK_a values are in our tested data range of 5.94−11.24. The acidity constant for cristobalite surface sites was calculated to be smaller than 5.94 (13). However, this inconsistency with the data presented here is likely due to the fact that the cristobalite surface structure is different from the amorphous SiO_2 used in this study, and/or the number density of high-acidity sites is relatively small. Although the surface acidity constant is estimated at a relatively wide range in this study, it is possible to narrow this range by carefully choosing probe molecules. As demonstrated in this study, SFG spectroscopy is capable of probing the proton transfer reactions between a well-defined single crystal mineral surface and the acidity-probe molecules. Although beyond the scope of this study, by carefully choosing two probe molecules with close acidity constants, we can potentially determine the pK_a values for single-crystal mineral surfaces within the accuracy range (± 1.0) of the theoretical calculations. In addition, an SFG system with the capability of obtaining vibrational information in the fingerprint region (800−1400 cm^{-1}) will greatly improve the ability to monitor the proton transfer reaction because of the richness of the distinctive peaks in this region. These studies are currently underway in our lab.

Acknowledgments

Supporting Information Available

Details of the sum frequency generation system setup and orientation angle calculations. This material is available free of charge via the Internet at http://pubs.acs.org.

Literature Cited

(1) Stumm, W.; Furrer, G. The Dissolution of Oxides and Aluminum Silicates: Examples of Surface Coordination-Controlled Kinetics. In *Aquatic Surface Chemistry*; Stumm, W., Ed.; Wiley-Interscience: New York, 1987.

(2) Usher, C. R.; Michel, A. E.; Grassian, V. H. Reactions on Mineral Dust. *Chem. Rev.* **2003**, *103* (12), 4883.

(3) Al-Abadleh, H. A.; Grassian, V. H. Oxide Surfaces as Environmental Interfaces. *Surf. Sci. Rep.* **2003**, *52* (3−4), 63.

(4) Myneni, S. C. B. Soft X-ray Spectroscopy and Spectromicroscopy of Organic Molecules in the Environment. *Rev. Min. Geochem.* **2002**, *49*, 485.

(5) Langmuir, D. *Aqueous Environmental Geochemistry*, 1st ed.; Pearson Education: Upper Saddle River, NJ, 1997.

(6) Stumm, W.; Morgan, J. J. *Aquatic Chemistry*, 3rd ed.; John Wiley & Sons: New York, 1996.

(7) Iler, R. K. *The Chemistry of Silica: Solubility, Polymerization, Colloid and Surface Properties, and Biochemistry*; John Wiley & Sons: New York 1979.

(8) Morrow, B. A.; Gay, I. D. Infrared and NMR Characterization of the Silica Surface. In *Adsorption on Silica Surface*; Papirer, E., Ed.; Marcel Dekker: New York. 2000.

(9) Elzinga, E. L.; Peak, D.; Sparks, D. L. Spectroscopic Studies of Pb(II)-Sulfate Interactions at the Goethite-Water Interface. *Geochim. Cosmochim. Acta* **2001**, *65* (14), 2219.

(10) Peak, D.; Luther, G. W.; Sparks, D. L. ATR-FTIR Spectroscopic Studies of Boric Acid Adsorption on Hydrous Ferric Oxide. *Geochim. Cosmochim. Acta* **2003**, *67* (14), 2552.

(11) Brown, G. E., Jr.; Henrich, V. E.; Casey, W. H.; Clark, D. L.; Eggleston, C.; Felmy, A.; Goodman, D. W.; Graetzel, M.; Maciel, G.; McCarthy, M. I.; Nealson, K. H.; Sverjensky, D. A.; Toney, M. F.; Zachara, J. M. Metal Oxide Surfaces and Their Interactions with Aqueous Solutions and Microbial Organisms. *Chem. Rev.* **1999**, *99* (9), 77.

(12) Morel, F. M. M.; Hering, J. G. *Principles and Applications of Aquatic Chemisty*. Wiley-Interscience: New York, 1993.

(13) Bickmore, B. R.; Tadanier, C. J.; Rosso, K. M.; Monn, W. D.; Eggett, D. L. Bond-Valence Methods for pK_a Prediction: Critical Reanalysis and a New Approach. *Geochim. Cosmochim. Acta* **2004**, *68* (9), 2025.

(14) Davis, J. A.; Kent, D. Surface Complexation Modeling in Aqueous Geochemistry. *Rev. Mineral.* **1990**, *23*, 177.

(15) Hiemstra, T.; Venema, P.; van Riemsdijk, W. H. Intrinsic Proton Affinity of Reactive Surface Groups of Metal (Hydr)Oxides: The Bond Valence Principle. *J. Colloid Interface Sci.* **1996**, *184* (2), 680.

(16) Paukshtis, E. A.; Yurchenko, E. N. Study of the Acid−Base Properties of Heterogeneous Catalysts by Infrared Spectroscopy. *Russ. Chem. Rev. (Engl. Transl.)* **1983**, *52*, 242.

(17) Parry, E. P. An Infrared Study of Pyridine Adsorbed on Acidic Solids. Characterization of Surface Acidity. *J. Catal.* **1963**, *2*, 371.

(18) Knozinger, H. in *Advances in Catalysis*, D. D. Eley; Pines, H.; Weisz, P. B., Editors. Academic Press: New York, 1976; p 184.

(19) Morterra, C.; Cerrato, G.; Meligrana, G. Revisiting the Use of 2,6-Dimethylpyridine Adsorption as a Probe for the Acidic Properties of Metal Oxides. *Langmuir* **2001**, *17* (22), 7053.

(20) Zaki, M. I.; Hasan, M. A.; Al-Sagheer, F. A.; Pasupulety, L. In Situ FTIR Spectra of Pyridine Adsorbed on $SiO_2-Al_2O_3$, TiO_2, ZrO_2 and CeO_2: General Considerations for the Identification of Acid Sites on Surfaces of Finely Divided Metal Oxides. *Colloid Surf.* **2001**, *190*, 261.

(21) Dines, T. J.; MacGregor, L. D.; Rochester, C. H. Adsorption of 2-Chloropyridine on Oxide−an Infrared Spectroscopic Study. *Spectrochim. Acta, Part A* **2003**, *59*, 3205.

(22) Rustard, J. R.; Wasserman, E.; Felmy, A. R.; Wilke, C. Molecular Dynamics Study of Proton Binding to Silica Surface. *J. Colloid Interface Sci.* **1998**, *198*, 119.

(23) Tsyganenko, A. A.; Storozheva, E. N.; Manoilova, O. V.; Lesage, G.; Daturi, M.; Lavalley, J.-C. Bronsted Acidity of Silica Silanol Group Induced by Adsorption of Acids. *Catal. Lett.* **2000**, *70*, 159.

(24) Miranda, P. B.; Shen, Y. R. Liquid Interfaces: A Study by Sum-Frequency Vibrational Spectroscopy. *J. Phys. Chem. B* **1999**, *103*, 3292.

(25) Shen, Y. R. *The Principles of Nonlinear Optics*, 1st ed.; John Wiley & Sons: New York, 1984.

(26) Al-Abadleh, H. A.; Voges, A. B.; Bertin, P. A.; Nguyen, S. T.; Geiger, F. M. Chromium(VI) Binding to Functionalized Silica/Water Interfaces Studied by Nonlinear Optical Spectroscopy. *J. Am. Chem. Soc.* **2004**, *126* (36), 11126.

(27) Bloembergen, N.; Pershan, P. S. Light Waves at the Boundary of Nonlinear Media. *Phys. Rev.* **1962**, *128* (2), 606.

(28) Hirose, C.; Akamatsu, N.; Domen, K. Formulas for the Analysis of the Surface SFG Spectrum and Transformation Coefficients of Cartesian SFG Tensor Components. *Appl. Spectrosc.* **1992**, *46* (6), 1051.

(29) Moad, A. J.; Simpson, G. J. A Unified Treatment of Selection Rules and Symmetry Relations for Sum-Frequency and Second Harmonic Spectroscopies. *J. Phys. Chem. B* **2004**, *108* (11), 3548.

(30) Shen, Y. R. Surface Contribution Versus Bulk Contribution in Surface Nonlinear Optical Spectroscopy. *Appl. Phys. B* **1999**, *68*, 295.

(31) Shultz, M. J.; Baldelli, S.; Schnitzer, C.; Simonelli, D. Aqueous Solution/Air Interfaces Probed with Sum Frequency Generation Spectroscopy. *J. Phys. Chem. B* **2002**, *106* (21), 5313.

(32) Richmond, G. L. Molecular Bonding and Interactions at Aqueous Surfaces as Probed by Vibrational Sum Frequency Spectroscopy. *Chem. Rev.* **2002**, *102* (8), 2693.

(33) Hommel, E. L.; Allen, H. C. 1-Methyl Naphthalene Reorientation at the Air−Liquid Interface Upon Water Saturation Studied by

Vibrational Broad Bandwidth Sum Frequency Generation Spectroscopy. *J. Phys. Chem. B* **2003**, *107*, 10823.

(34) Ma, G.; Allen, H. C. Diffuse Reflection Broad Bandwidth Sum Frequency Generation from Particle Surfaces. *J. Am. Chem. Soc.* **2002**, *124* (32), 9374.

(35) Liu, D.; Ma, G.; Levering, L. M.; Allen, H. C. Vibrational Spectroscopy of Aqueous Sodium Halide Solutions and Air−Liquid Interfaces: Observation of Increased Interfacial Depth. *J. Phys. Chem. B* **2004**, *108* (7), 2252.

(36) Liu, D.; Ma, G.; Xu, M.; Allen, H. C. Adsorption of Ethylene Glycol Vapor on α-Al$_2$O$_3$ (0001) and Amorphous SiO$_2$ Surfaces: Observation of Molecular Orientation and Surface Hydroxyl Groups as Sorption Sites. *Environ. Sci. Technol.* **2005**, *39* (1), 206.

(37) Long, D. A.; George, W. O. Spectroscopic and Thermodynamic Studies of Pyridine Compounds−Vibrational Spectra and Assignments for R−Picoline and R−Picoline-D7. *Spectrochim. Acta* **1963**, *19*, 1777.

(38) Arenas, J. F.; Lopez Tocon, I.; Otero, J. C.; Marcos, J. I. Vibrational Spectra of Methylpyridines. *J. Mol. Struct.* **1999**, *476*, 139.

(39) Kudoh, S.; Takayanagi, M.; Nakata, M. Infrared Spectra of Dewar 4-Picoline in Low-Temperature Argon Matrixes and Vibrational Analysis by DFT Calculation. *Chem. Phys. Lett.* **2000**, *322*, 363.

(40) Zhang, D.; Gutow, J.; Eisenthal, K. B. Vibrational Spectra, Orientations, and Phase Transitions in Long-Chain Amphiphiles at the Air/Water Interface: Probing the Head and Tail Groups by Sum Frequency Generation. *J. Phys. Chem.* **1994**, *98*, 13729.

(41) Lu, R.; Gan, W.; Wu, B.-H.; Chen, H.; Wang, H.-f. Vibrational Polarization Spectroscopy of CH Stretching Modes of the Methylene Group at the Vapor/Liquid Interfaces with Sum Frequency Generation. *J. Phys. Chem. B* **2004**, *108*, 7297.

(42) Davydov, V. Y. Adsorption on Silica Surfaces. In *Adsorption on Silica Surfaces*; Papirer, E, Ed.; Marcel Dekker: New York. 2000, p 63.

(43) Ma, G.; Liu, D.; Allen, H. C. Piperidine Adsorption on Hydrated α-Alumina (0001) Surface Studied by Vibrational Sum Frequency Generation Spectroscopy. *Langmuir* **2004**, *20* (26), 11620.

(44) Sanchez, L. A.; Birke, R. L.; Lombardi, J. R. Surface Enhanced Raman Scattering of Ammonia. *J. Phys. Chem.* **1984**, *88*, 1762.

(45) Titova, T. V.; Anisimova, O. S.; Pentin, Y. A. Vibrational Spectra of Piperidine and Its Simple Derivatives. III. Calculation of the Frequencies and Normal Vibrational Forms for Piperidine and N-Deuteriopiperidine. *Opt. Spectrosc. (Engl. Transl.)* **1967**, *32*, 495.

(46) Vedal, D.; Ellestad, O. H.; Klaboe, P. The Vibrational Spectra of Piperidine and Morpholine and Their N-Deuterated Analogues. *Spectrochim. Acta* **1976**, *32A*, 877.

(47) Krueger, P. J.; Jan, J. Conformational Equilibriums in Some Cyclic Imines: NH and CH Stretching Vibrations and the Axial Lone Pair. *Can. J. Chem.* **1970**, *48* (20), 3236.

(48) Diez, R. P.; Amalvy, J. I. A Density Functional Study of the Adsorption of Pyridine, 2-Vinylpyridine, and 4-Vinylpyridine onto a Silica Surface. *J. Mol. Struct.: THEOCHEM* **2003**, *634*, 187.

(49) Shenderovich, I. G.; Buntkowsky, G.; Schreiber, A.; Gedat, E.; Sharif, S.; Albrecht, J.; Golubev, N. S.; Findenegg, G. H.; Limbach, H.-H. Pyridine-^{15}N − a Mobile NMR Sensor for Surface Acidity and Surface Defects of Mesoporous Silica. *J. Phys. Chem. B* **2003**, *107* (43), 11924.

(50) Dines, T. J.; MacGregor, L. D.; Rochester, C. H. IR Spectroscopic Investigation of the Interaction of Quinoline with Acidic Sites on Oxide Surfaces. *Langmuir* **2002**, *18* (6), 2300.

(51) Dines, T. J.; MacGregor, L. D.; Rochester, C. H. Adsorption of 2-Chloropyridine on Oxides-an Infrared Spectroscopic Study. *Spectrochim. Acta, Part A* **2003**, *59A* (13), 3205.

(52) Dines, T. J.; MacGregor, L. D.; Rochester, C. H. The Surface Acidity of Oxides Probed by IR Spectroscopy of Adsorbed Diazines. *Phys. Chem. Chem. Phys.* **2001**, *3* (13), 2676.

(53) Dines, T. J.; MacGregor, L. D.; Rochester, C. H. IR Spectroscopy of *N*-Methylpyrrole Adsorbed on Oxides. A Probe of Surface Acidity. *J. Colloid Interface Sci.* **2002**, *245* (2), 221.